

General Disclaimer

One or more of the Following Statements may affect this Document

- This document has been reproduced from the best copy furnished by the organizational source. It is being released in the interest of making available as much information as possible.
- This document may contain data, which exceeds the sheet parameters. It was furnished in this condition by the organizational source and is the best copy available.
- This document may contain tone-on-tone or color graphs, charts and/or pictures, which have been reproduced in black and white.
- This document is paginated as submitted by the original source.
- Portions of this document are not fully legible due to the historical nature of some of the material. However, it is the best reproduction available from the original submission.

NASA TM X-56036

STABILITY AND CONTROL DERIVATIVES OF THE T-37B AIRPLANE

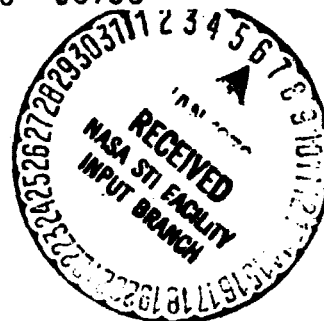
Mary F. Shafer

(NASA-TM-X-56036) STABILITY AND CONTROL
DERIVATIVES OF THE T-37B AIRPLANE (NASA)
31 p HC \$4.00 CSCL 01C

N76-14137

Unclas
G3/08 06788

September 1975



NASA high-number Technical Memorandums are issued to provide rapid transmittal of technical information from the researcher to the user. As such, they are not subject to the usual NASA review process.

NASA Flight Research Center
Edwards, California 93523

| | | | |
|---|---|--|------------|
| 1. Report No. TM X-56036 | 2. Government Accession No. | 3. Recipient's Catalog No. | |
| 4. Title and Subtitle STABILITY AND CONTROL DERIVATIVES OF THE T-37B AIRPLANE | | 5. Report Date September 1975 | |
| | | 6. Performing Organization Code | |
| 7. Author(s) Mary F. Shafer | | 8. Performing Organization Report No. | |
| | | 10. Work Unit No. 512-53-03 | |
| 9. Performing Organization Name and Address NASA Flight Research Center P.O. Box 273 Edwards, California 93523 | | 11. Contract or Grant No. | |
| | | 13. Type of Report and Period Covered Technical Memorandum | |
| 12. Sponsoring Agency Name and Address National Aeronautics and Space Administration Washington, D.C. 20546 | | 14. Sponsoring Agency Code | |
| | | 15. Supplementary Notes | |
| 16. Abstract <p style="text-align: center;">Subsonic stability and control derivatives were determined by a modified maximum likelihood estimator from flight data for the longitudinal and lateral-directional modes of the T-37B airplane. Data from two flights, in which 166 stability and control maneuvers were performed, were used in the determination. Four configurations of the airplane were investigated. The configurations were zero flaps, gear up; half flaps, gear up; full flaps, gear up; and zero flaps, gear down.</p> | | | |
| 17. Key Words (Suggested by Author(s)) T-37B airplane Stability and control derivatives | | 18. Distribution Statement Unclassified - Unlimited | |
| 19. Security Classif. (of this report) Unclassified | 20. Security Classif. (of this page) Unclassified | 21. No. of Pages 30 | 22. Price* |

STABILITY AND CONTROL DERIVATIVES
OF THE T-37B AIRPLANE

Mary F. Shafer
Flight Research Center

INTRODUCTION

Because of the continuing interest in flight simulation and handling qualities, there is a requirement for reliable estimates of the stability and control derivatives of most types of aircraft. In response to these requirements, the NASA Flight Research Center perfected a technique for minimizing the effort of determining the stability and control derivatives of aircraft from flight data (ref. 1) and developed a set of FORTRAN computer programs to implement the technique (ref. 2). The method of derivative extraction is based on a modified maximum likelihood estimator that uses the Newton-Raphson algorithm to perform the required minimization.

These computer programs are currently being used at the Flight Research Center to obtain stability and control derivatives for a wide variety of aircraft. Among the aircraft studied is the T-37B airplane, a small jet trainer. This report presents the estimates of the derivatives for the T-37B airplane determined by the modified maximum likelihood estimation technique from flight data.

These flight data were selected from maneuvers performed in the course of a multiple purpose flight test program. As a result, the entire flight envelope was not studied in the flight test program. In some instances, the incremental effect of a configuration was studied instead of all possible configurations.

SYMBOLS

| | |
|-------|-----------------------------|
| C_l | rolling-moment coefficient |
| C_m | pitching-moment coefficient |
| C_N | normal-force coefficient |

| | |
|------------|--|
| C_{N_0} | normal-force coefficient for zero angle of attack and zero elevator deflection |
| C_n | yawing-moment coefficient |
| C_Y | side-force coefficient |
| p | roll rate, deg/sec or rad/sec |
| q | pitch rate, deg/sec or rad/sec |
| r | yaw rate, deg/sec or rad/sec |
| α | angle of attack with respect to body axes, deg or rad |
| β | angle of sideslip, deg or rad |
| δ_a | aileron deflection, deg or rad |
| δ_e | elevator deflection, deg or rad |
| δ_r | rudder deflection, deg or rad |

Subscripts:

$p, q, r, \alpha, \beta, \delta_a, \delta_e, \delta_r$ partial derivative with respect to the subscripted variable

DESCRIPTION OF THE AIRPLANE AND INSTRUMENTATION

The T-37B airplane (figs. 1 and 2) is a small two seat twin engine subsonic jet with a low wing and retractable landing gear. The primary control surfaces are ailerons, elevators, and rudder. The airplane also has flaps and a speed brake, but the effect of the speed brake was not investigated in this study. Details and specifications for the airplane are given in reference 3.

Airspeed, altitude, and the pertinent stability and control quantities were among the data recorded. Angles of attack and sideslip were measured by vanes on a nose boom. Data were acquired by means of a pulse code modulation (PCM) system, which converts analog signals to digital format. Standard passive analog filters at 40 hertz were applied to all the data signals. The digital data were recorded on magnetic tape and telemetered to a ground station for real time monitoring and recording.

TEST PROCEDURE AND FLIGHT CONDITIONS

Data were gathered from two flights in which a total of 166 stability and control maneuvers were performed. Of these maneuvers, 73 were performed primarily with elevator input, 51 were performed primarily with aileron input, and 42 were performed primarily with rudder input. The maneuvers were performed so that the linearity of the airplane model could be maintained. Thus, the airplane was flown at a stabilized flight condition before the pilot initiated the control input for the maneuver. The pilot inputs approximated doublets. The peak to peak amplitudes of the control inputs ranged from 5° to 15° for elevator deflection, from 20° to 30° for aileron deflection, and from 20° to 50° for rudder deflection.

Four airplane configurations were investigated. The configurations were zero flaps, gear up; half flaps, gear up; full flaps, gear up; and zero flaps, gear down.

METHOD OF ANALYSIS

A maximum likelihood estimator method of analysis was used to determine a complete set of linear stability and control derivatives from the maneuvers performed in flight. This method is called the modified maximum likelihood estimator and is fully described in reference 1. The method, sometimes called the Newton-Raphson method, is an iterative technique that minimizes the difference between the measured aircraft response and the computed aircraft response by adjusting the stability and control derivative values used in calculating the computed response. The Newton-Raphson algorithm was used to obtain the minimizations. The method can be modified to include *a priori* information from previous calculations, flight tests, or wind-tunnel tests. This modification is made by including a penalty for adjusting the unknown stability and control derivatives away from the *a priori* values. If new information is contained in a flight maneuver, the estimate of the derivative is affected only slightly by the *a priori* information. If no new information is contained in a maneuver, however, the *a priori* value results. A complete description of the computer program used for the derivative extraction and FORTRAN listings are given in reference 2.

In addition to giving estimates of the derivatives, this method of analysis provides uncertainty levels for each derivative. The uncertainty levels are proportional to the approximation of the Cramèr-Rao bounds described in reference 1 and are analogous to the standard deviations of the estimated derivatives. The larger the uncertainty level, the more uncertain the validity of the estimated value. The uncertainty levels obtained for a derivative from different maneuvers at the same flight condition can be compared to determine the most valid. Therefore, the uncertainty levels provide additional information about the validity of the estimate of the derivative.

RESULTS AND DISCUSSION

Four maneuvers yielded completely unsatisfactory fits. The results of these maneuvers, two of which were performed with aileron inputs and two with rudder in-

puts, are not presented. As a result, estimates from 162 maneuvers (98 percent of those flown) are presented; 73 performed primarily with elevator input, 49 performed primarily with aileron input, and 40 performed primarily with rudder input.

The zero flaps, gear up basic configuration is the most common in normal flight and is therefore presented as the basis for comparison in figures 3 to 6. Many basic configuration maneuvers produced estimates with nearly identical values for angles of attack from 2° to 3° . Not all these nearly identical values are presented in figures 4 and 6.

The longitudinal stability and control derivative estimates are presented in figures 3 and 4, and the lateral-directional derivative estimates are shown in figures 5 and 6. The symbol shows the value of the derivative for each maneuver, and the vertical bar associated with each symbol represents the uncertainty level for that estimate. The estimates of C_N and $\delta_{e\text{trim}}$ do not have uncertainty levels, since they are calculated from other estimates. Not all control derivatives are plotted for all maneuvers, because control derivatives can be estimated only when that control varies during the maneuver, and for some maneuvers only one control varied.

Longitudinal Derivatives

The estimates of the longitudinal stability and control derivatives for the gear up and gear down configurations with zero flaps are shown in figure 3. Gear position had virtually no effect on C_{N_α} . The changes due to gear position in all the other derivative estimates are apparent in figure 3.

The effects of the various flap settings with gear up are shown in figure 4. Flap position had virtually no effect on C_{m_q} . All other derivatives show more marked changes. The data indicate that there is little difference for most of the derivatives between the effects of half and full flaps. The zero, half, and full flap settings result in significantly different estimates for the normal-force coefficient, C_N . However, all three fairings have approximately the same slope when C_N is plotted against angle of attack. The coefficient C_N is calculated from C_{N_α} , $C_{N_{\delta_e}}$, and C_{N_0} . The values of C_{N_0} vary most with flap setting and cause most of the offsets in C_N .

Lateral-Directional Derivatives

The lateral-directional stability and control derivatives for the gear up and gear down configurations with zero flaps are presented in figure 5. The derivatives C_{l_β} , C_{n_p} , C_{n_r} , $C_{n_{\delta_a}}$, $C_{l_{\delta_r}}$, $C_{Y_{\delta_r}}$, and $C_{Y_{\delta_a}}$ are not markedly affected by gear posi-

tion. The estimates of the other derivatives are affected by gear position.

The estimates for the various flap settings with gear up are presented in figure 6. The derivatives $C_{Y\beta}$, $C_{n\delta_a}$, $C_{l\delta_r}$, $C_{Y\delta_r}$, and $C_{Y\delta_a}$ are not significantly affected by the position of the flaps. Only $C_{l\delta_a}$ shows much difference between half and full flaps. For the other derivatives, as in the longitudinal cases, the amount of the deflection of the flaps does not have a notable effect.

Fairings

The fairings of most of the stability and control derivatives are based solely on the estimates and the uncertainty levels associated with each of the estimates. In figures 5(f) and 6(f), the fairings of $C_{l\delta_r}$ are not consistent with all of the data shown. These fairings were determined from the quality of the comparison between the computed roll rate and the measured roll rate for the portion of the maneuver where the rudder was varying. The $C_{l\delta_r}$ estimates near the fairings resulted from maneuvers where the comparison between the responses was good.

CONCLUDING REMARKS

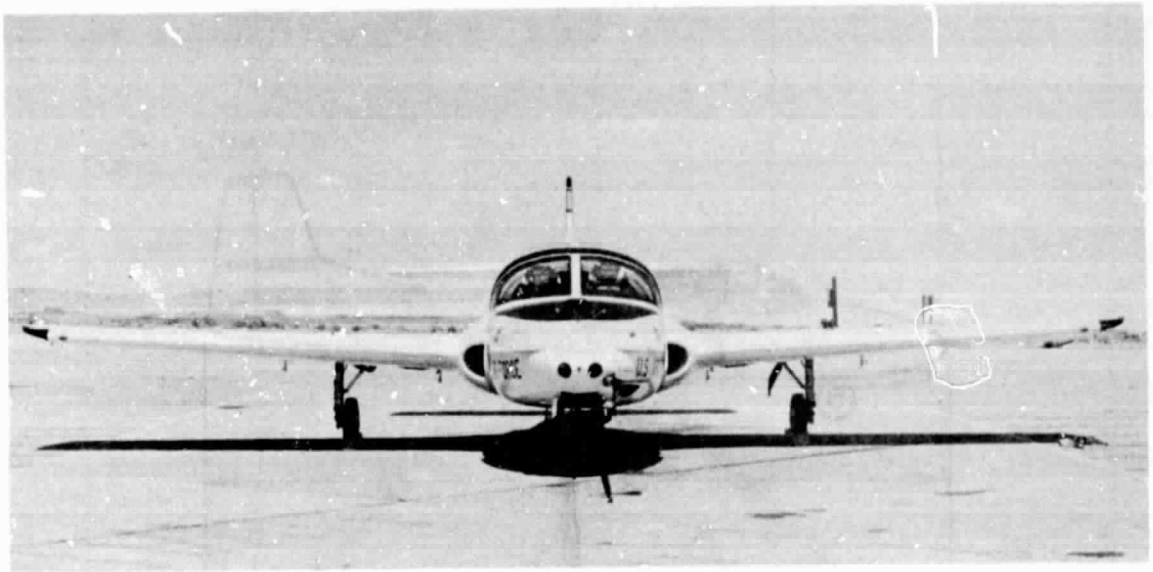
A complete set of the linear stability and control derivatives of the T-37B airplane was determined with a modified maximum likelihood estimator. The derivatives were extracted from subsonic flight data from two flights for the longitudinal and lateral-directional modes. Four airplane configurations were investigated: zero flaps, gear up; half flaps, gear up; full flaps, gear up; and zero flaps, gear down. Of the 166 maneuvers flown, 98 percent yielded satisfactory results.

The data indicate that the amount of flap deflection has a significant effect on the magnitude of the stability and control derivatives, although half and full flaps caused similar changes in most of the derivatives. Some of the significant derivatives were affected by the position of the gear.

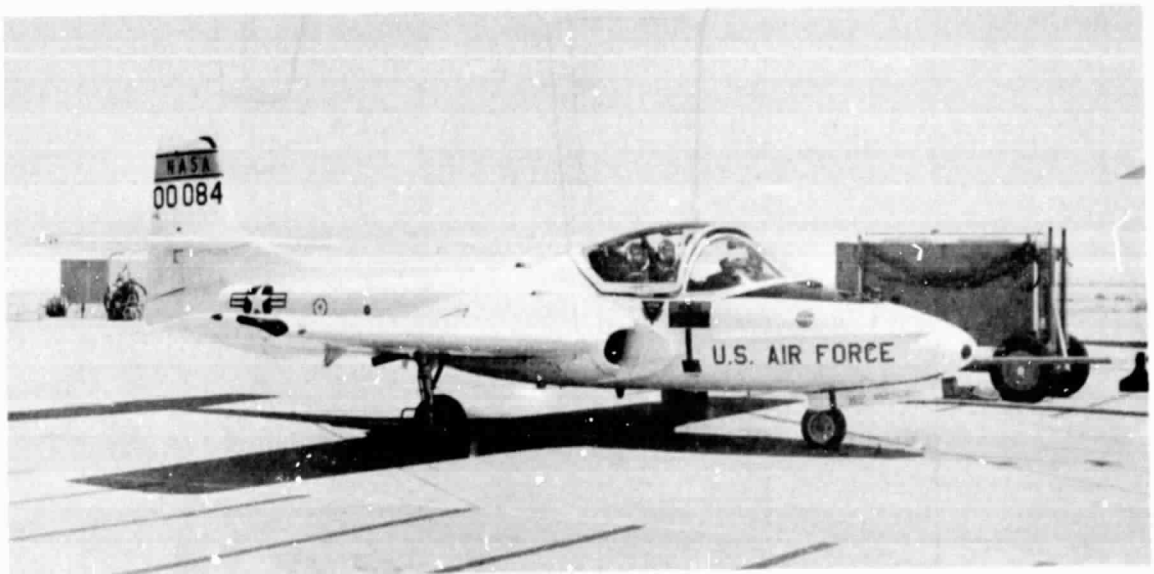
*Flight Research Center
National Aeronautics and Space Administration
Edwards, California 93523
September 11, 1975*

REFERENCES

1. Iliff, Kenneth W.; and Taylor, Lawrence W., Jr.: Determination of Stability Derivatives From Flight Data Using a Newton-Raphson Minimization Technique. NASA TN D-6579, 1972.
2. Maine, Richard E.; and Iliff, Kenneth W.: A FORTRAN Program for Determining Aircraft Stability and Control Derivatives From Flight Data. NASA TN D-7831, 1975.
3. Smith, Harriet J.: A Flight Test Investigation of the Rolling Moments Induced on a T-37B Airplane in the Wake of a B-747 Airplane. NASA TM X-56031, 1975.



E-28886



E-28887

**ORIGINAL PAGE IS
OF POOR QUALITY**

Figure 1. T-37B airplane.

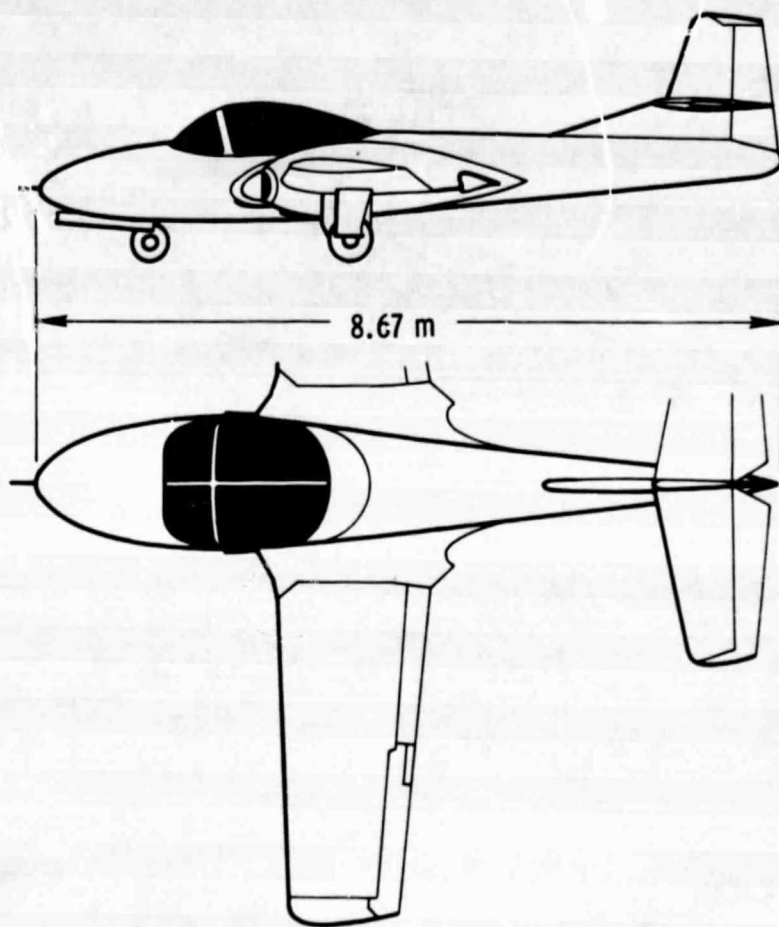
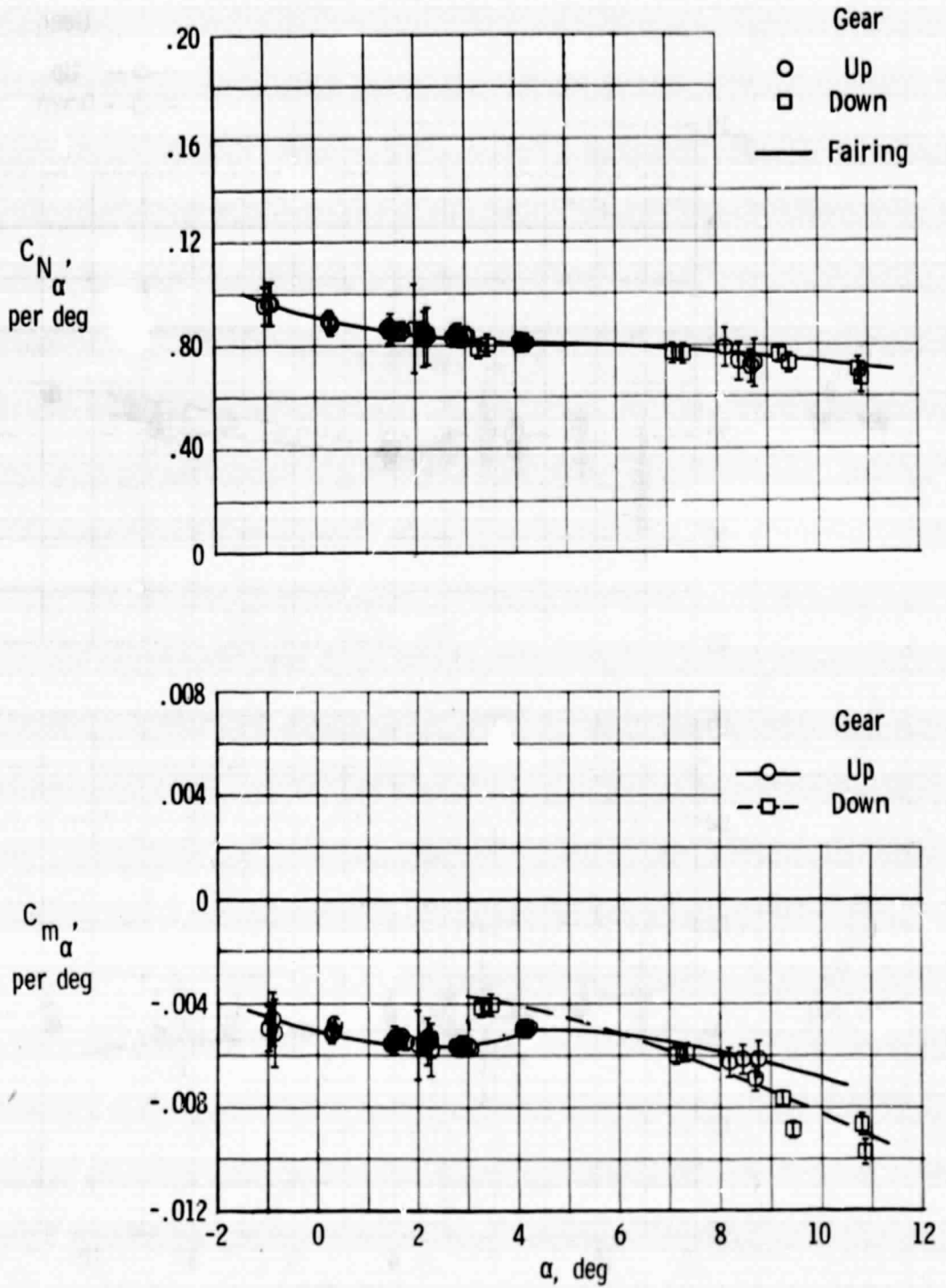


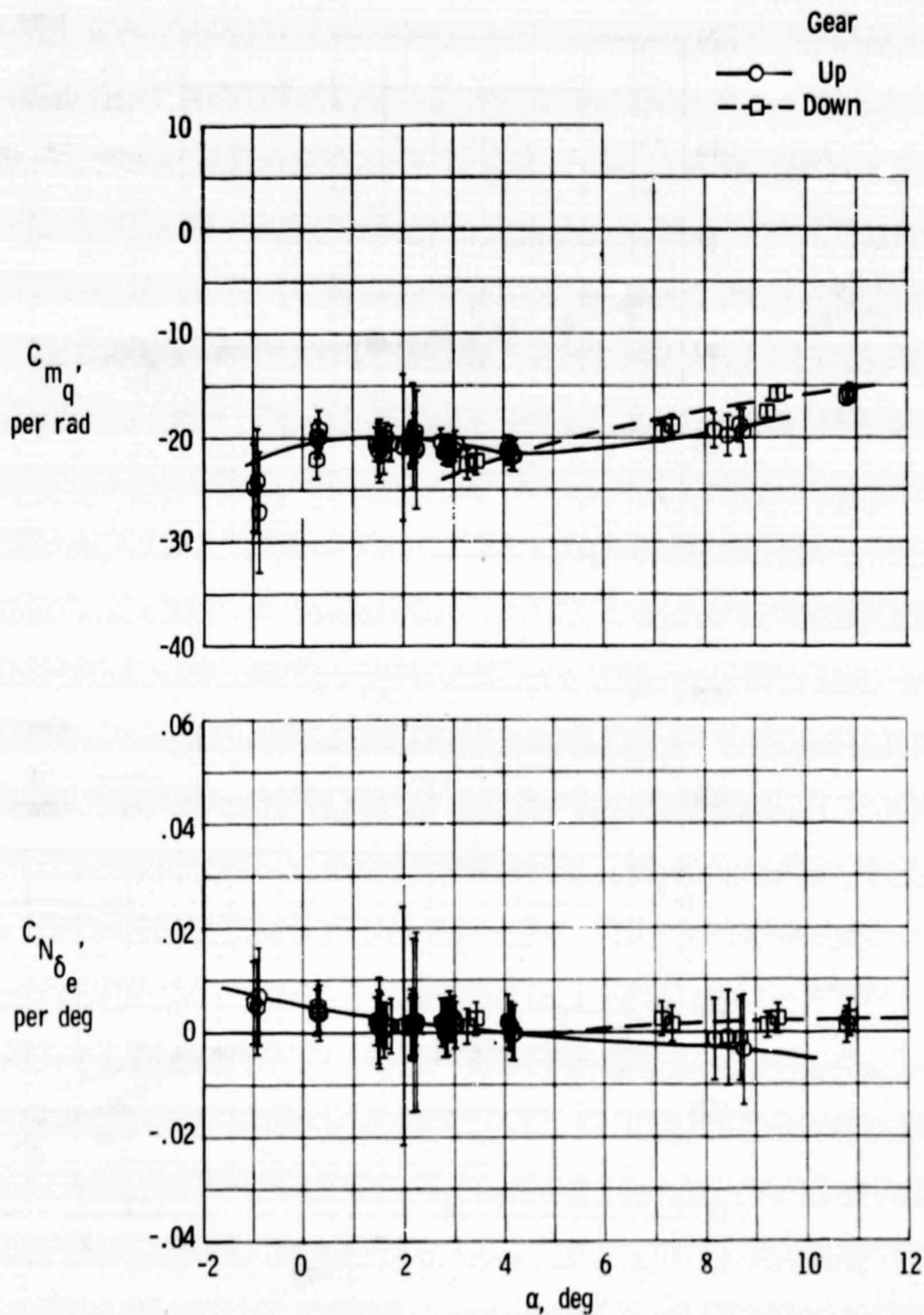
Figure 2. Two-view drawing of T-37B airplane.

FORM 1-62
GPO : 1962 O - 348-000



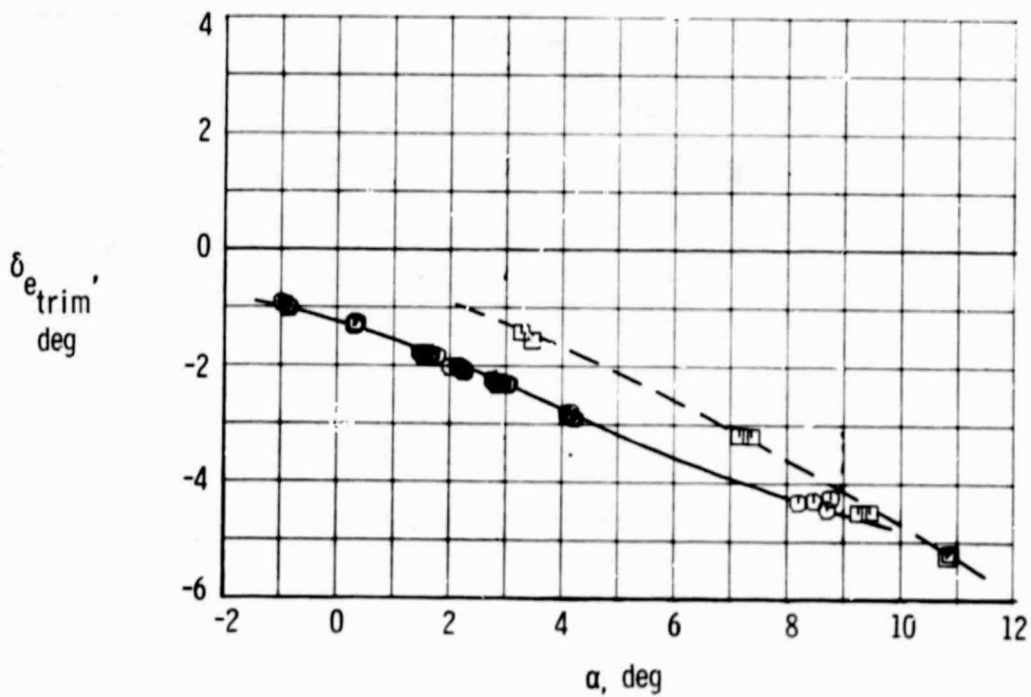
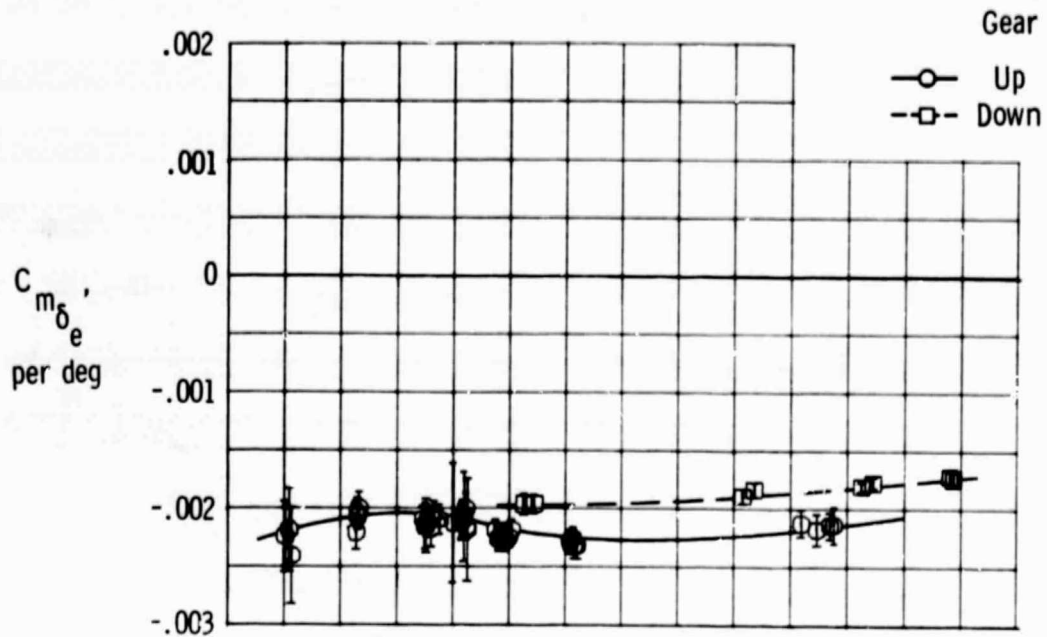
(a) C_{N_α} , C_{m_α} .

Figure 3. Longitudinal stability and control derivatives for zero flap configurations.



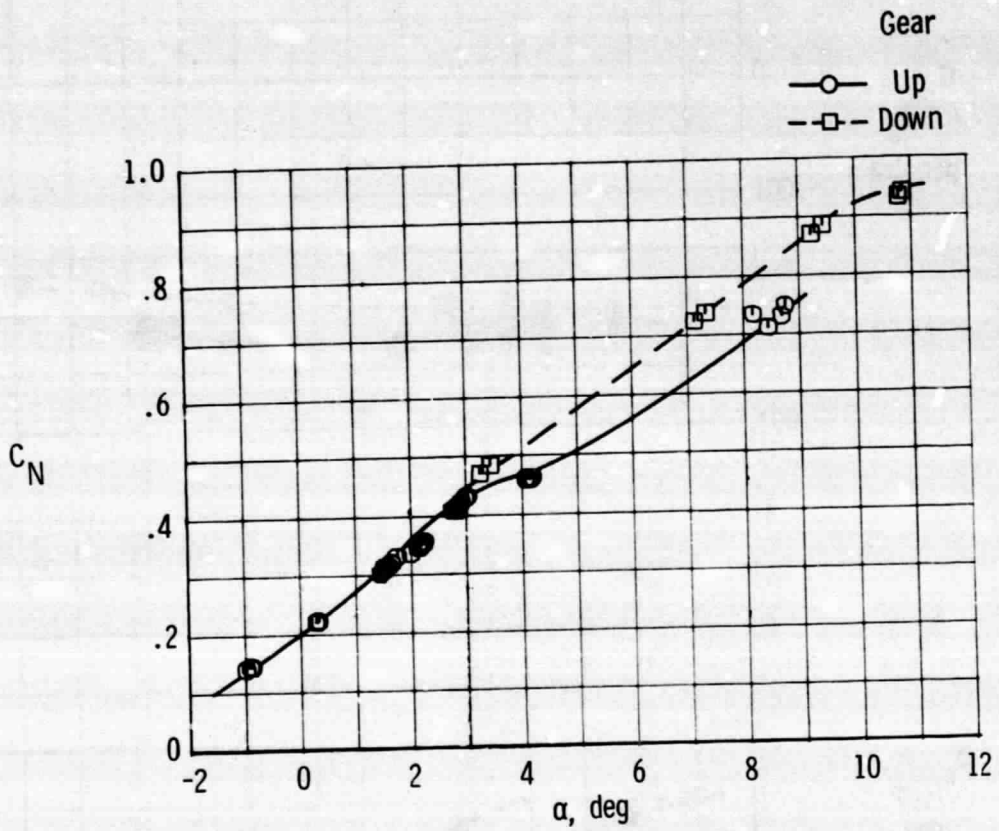
(b) C_{m_q} , $C_{N_{\delta_e}}$

Figure 3. Continued.



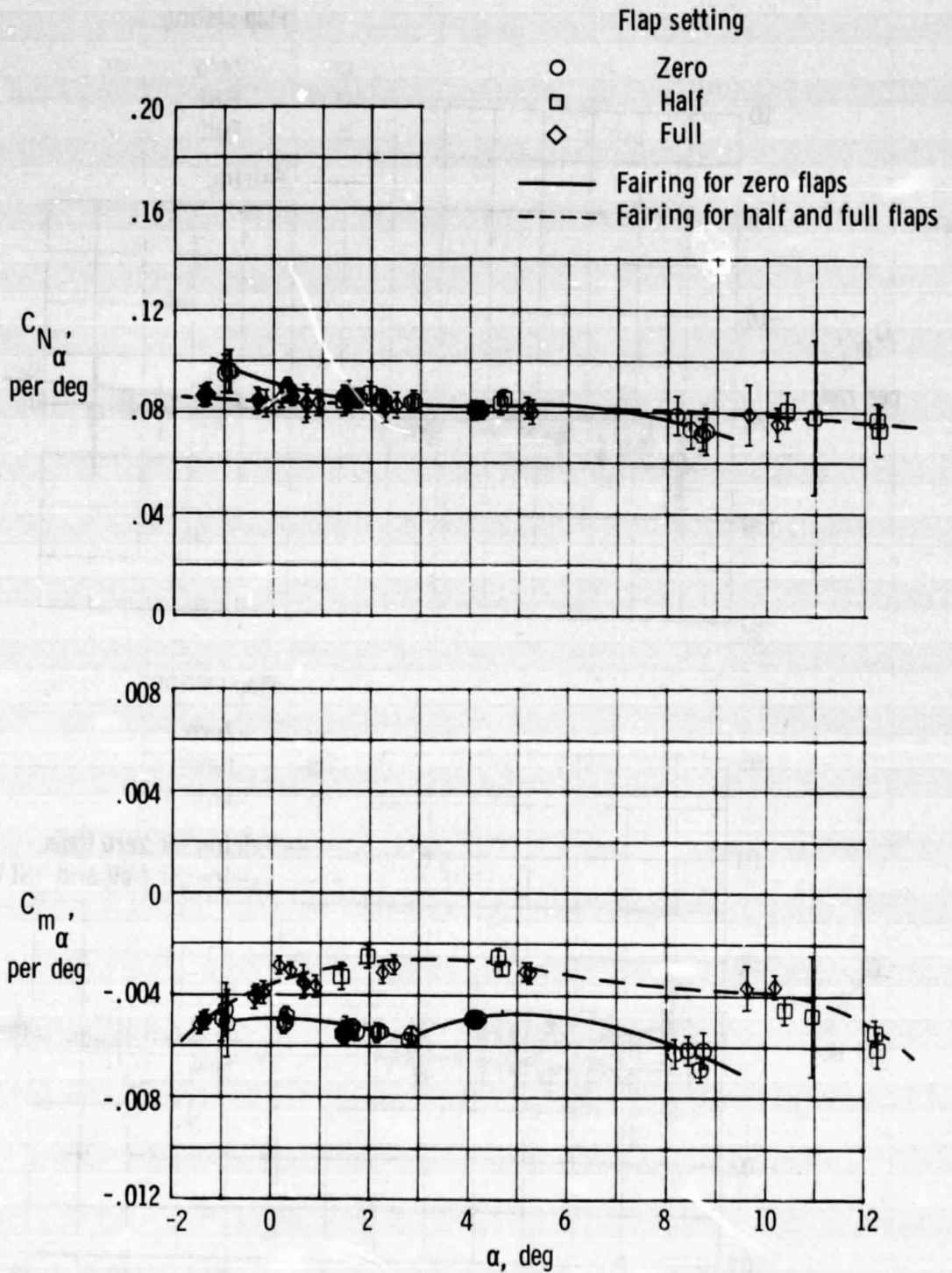
(c) $C_{m_{\delta_e}}$, $\delta_{e_{trim}}$

Figure 3. Continued.



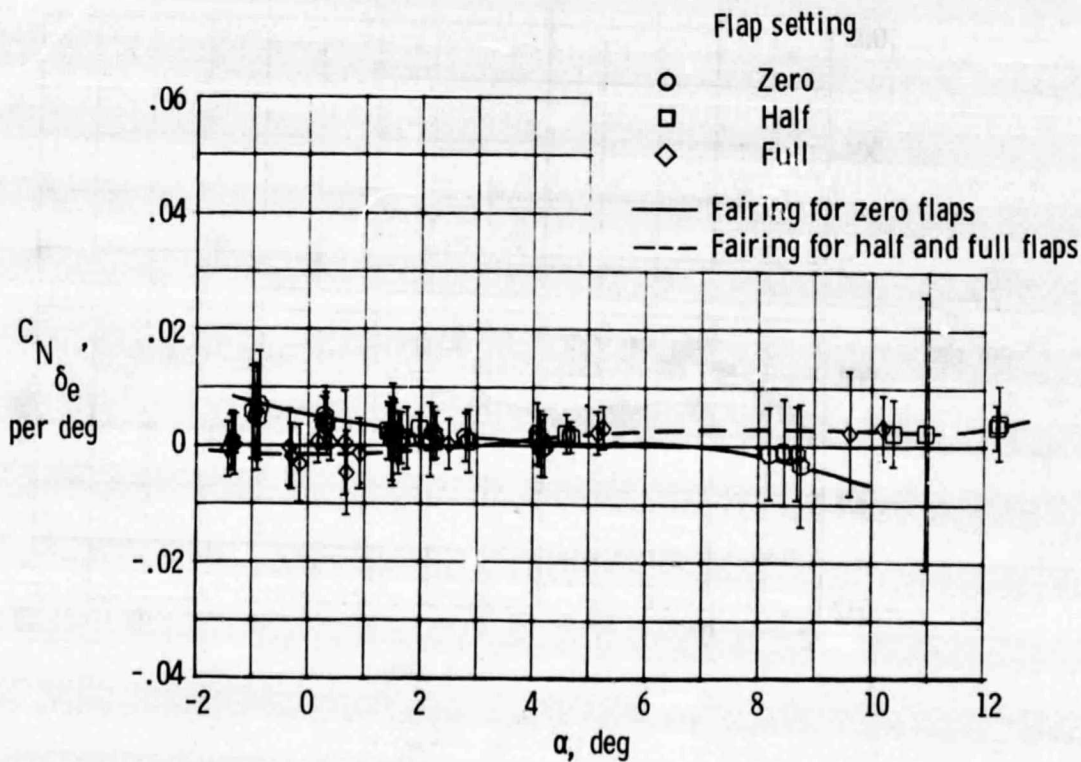
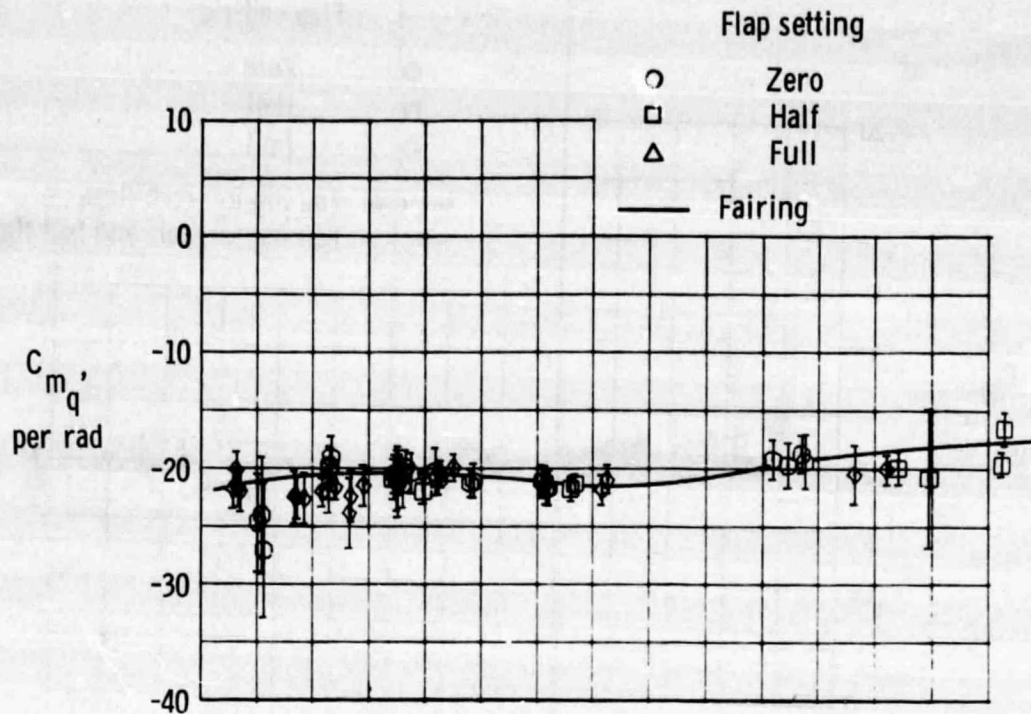
(d) C_N .

Figure 3. Concluded.



(a) C_{N_α} , C_{m_α}

Figure 4. Longitudinal stability and control derivatives for gear up configurations.



(b) $C_{m_q}, C_{N_{\delta_e}}$

Figure 4. Continued.

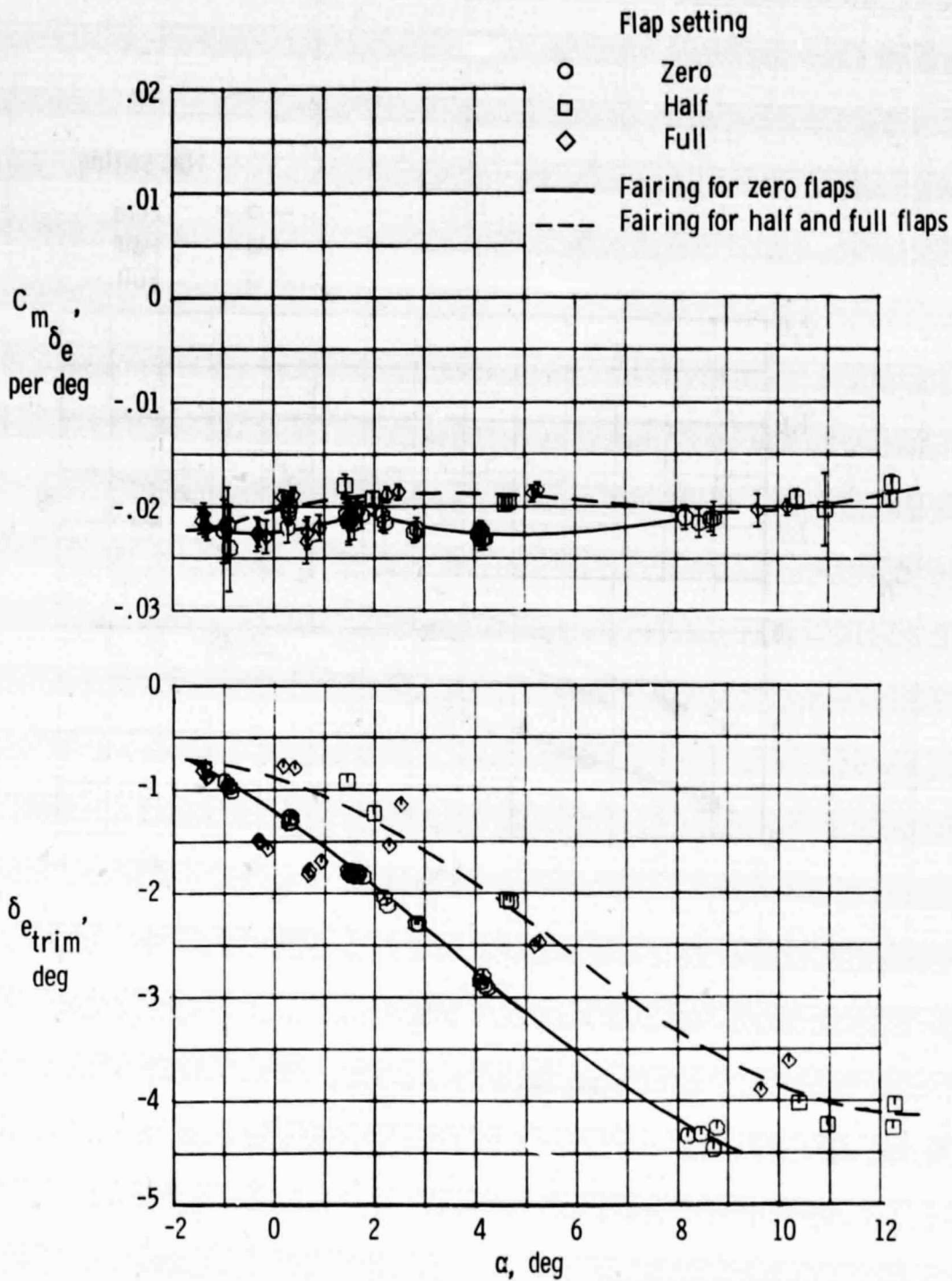
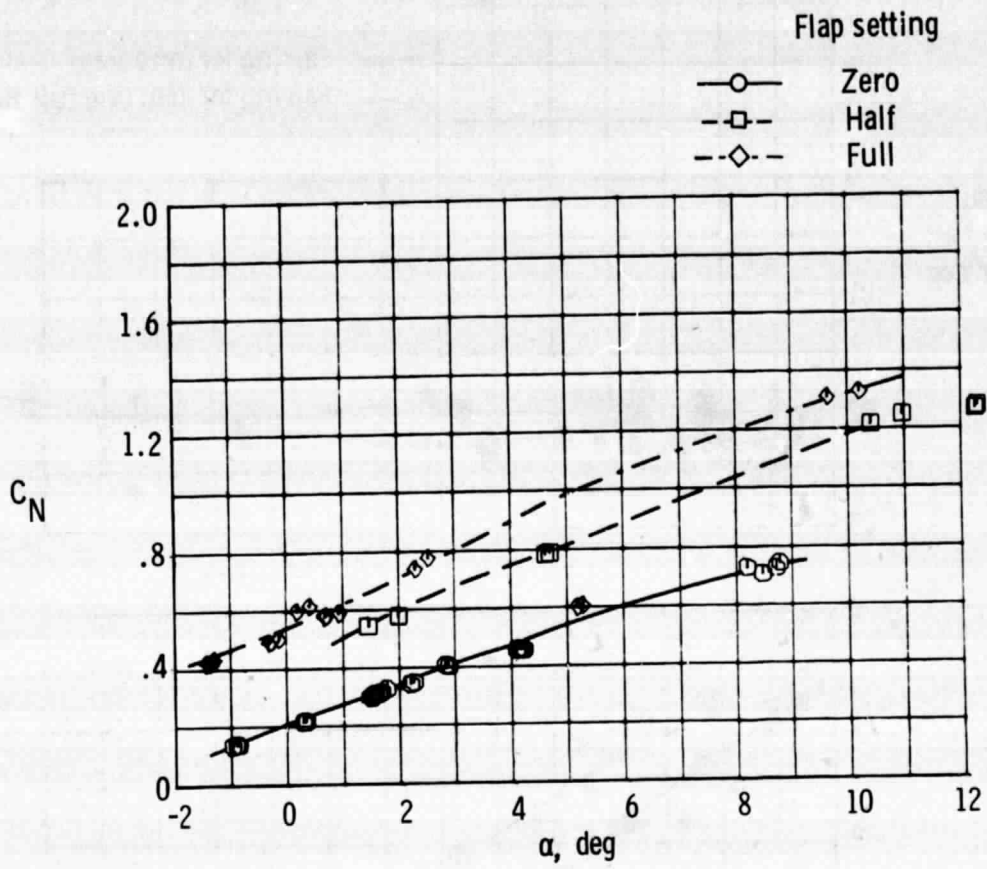


Figure 4. Continued.



(d) C_N .

Figure 4. Concluded.

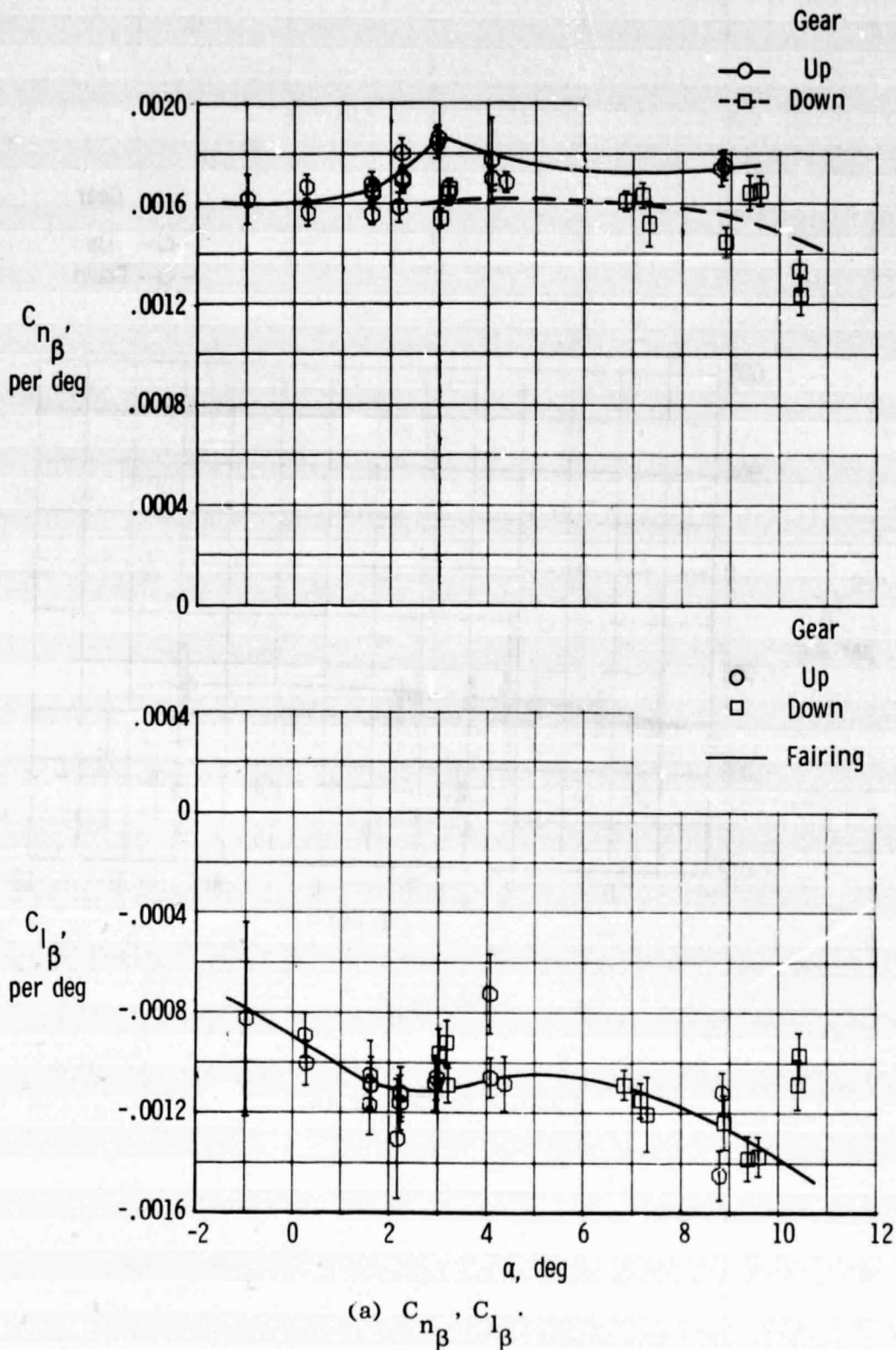
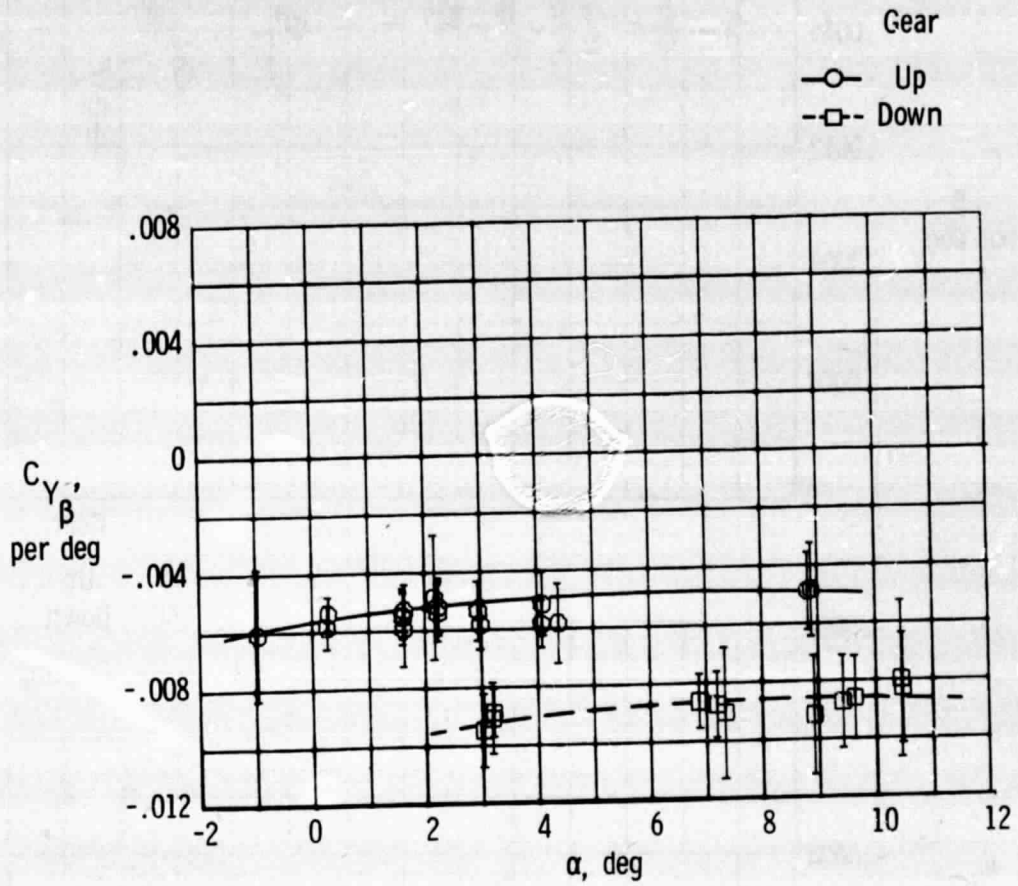
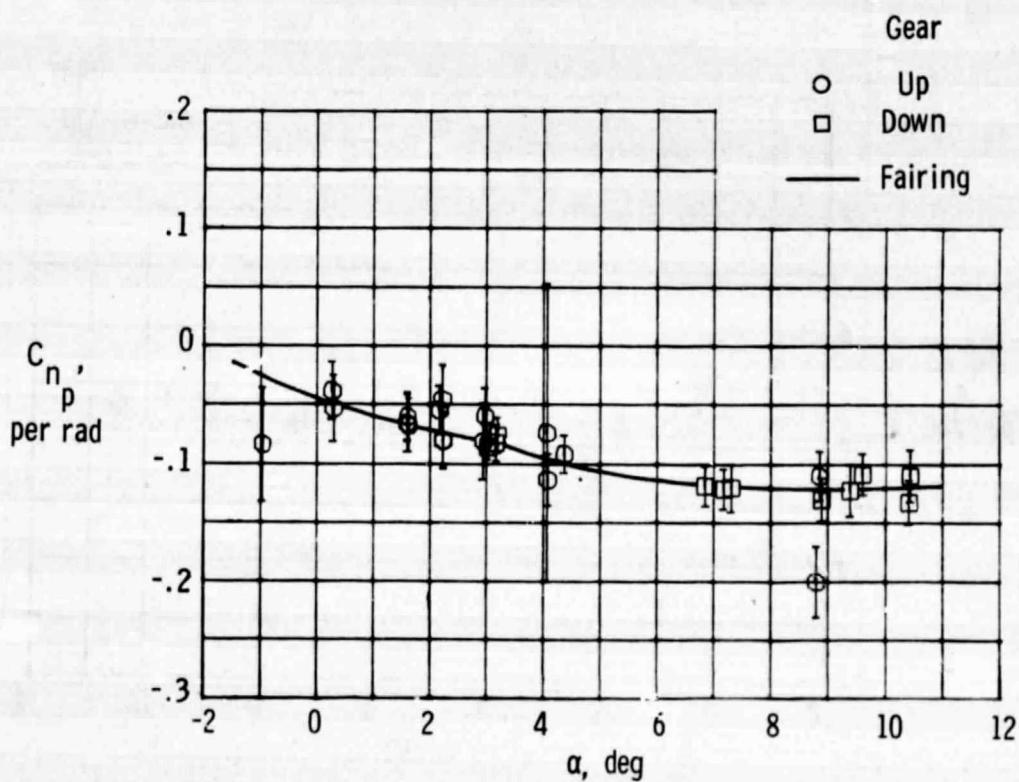
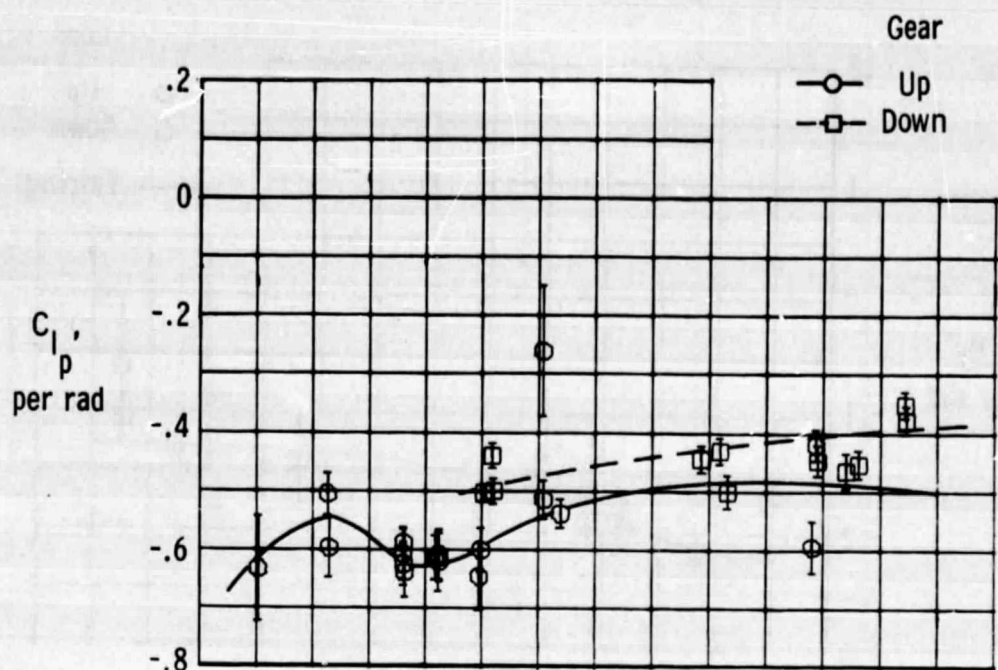


Figure 5. Lateral-directional stability and control derivatives for zero flap configurations.



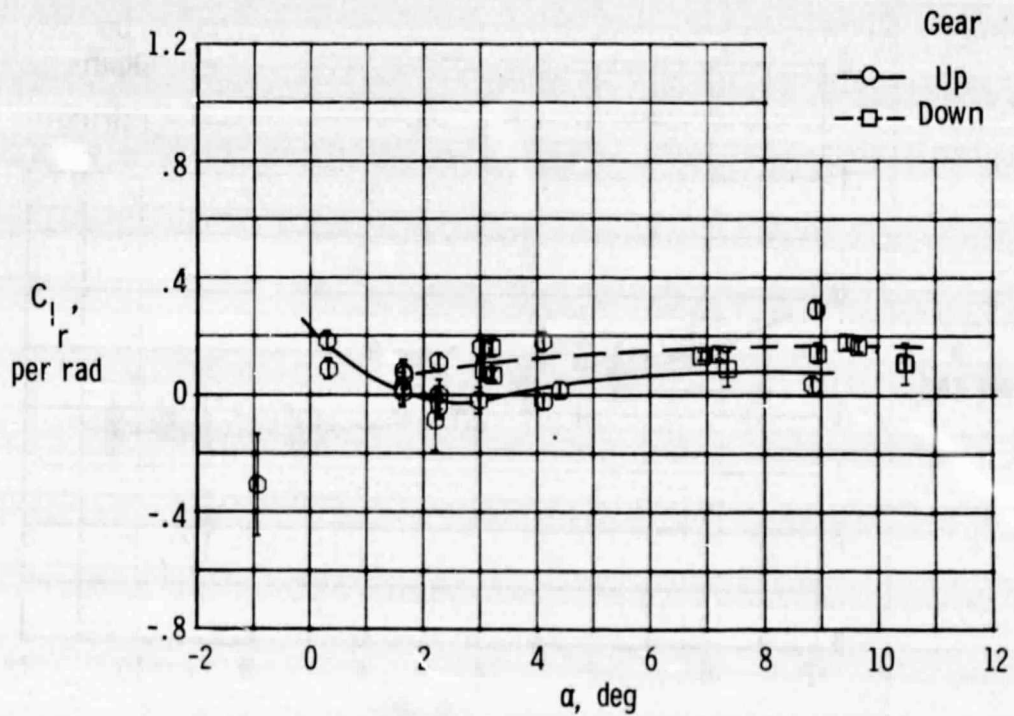
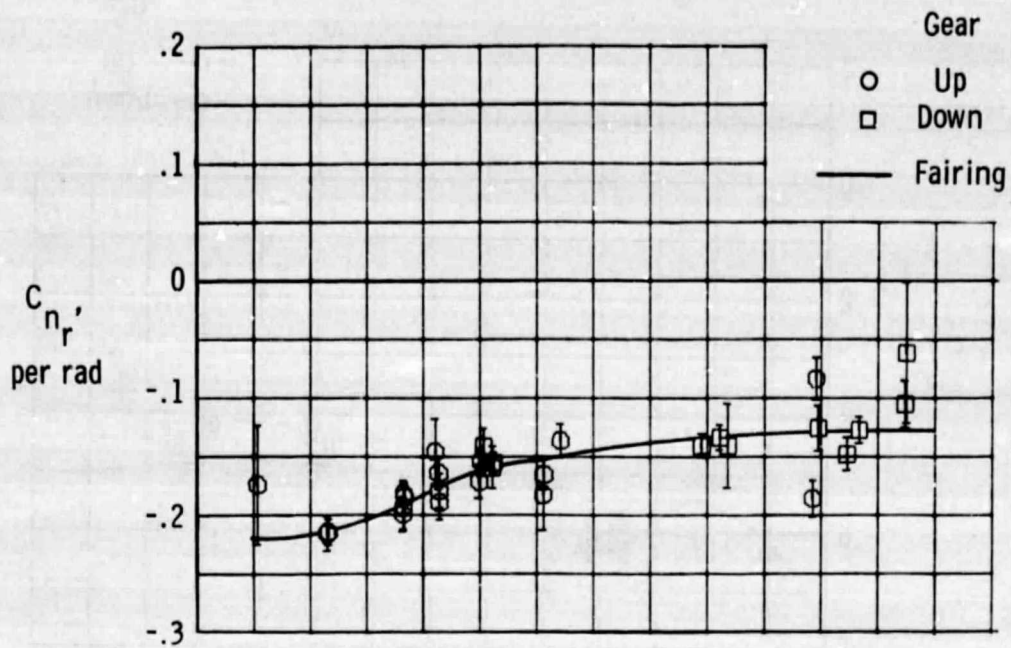
(b) $C_{Y\beta}$.

Figure 5. Continued.



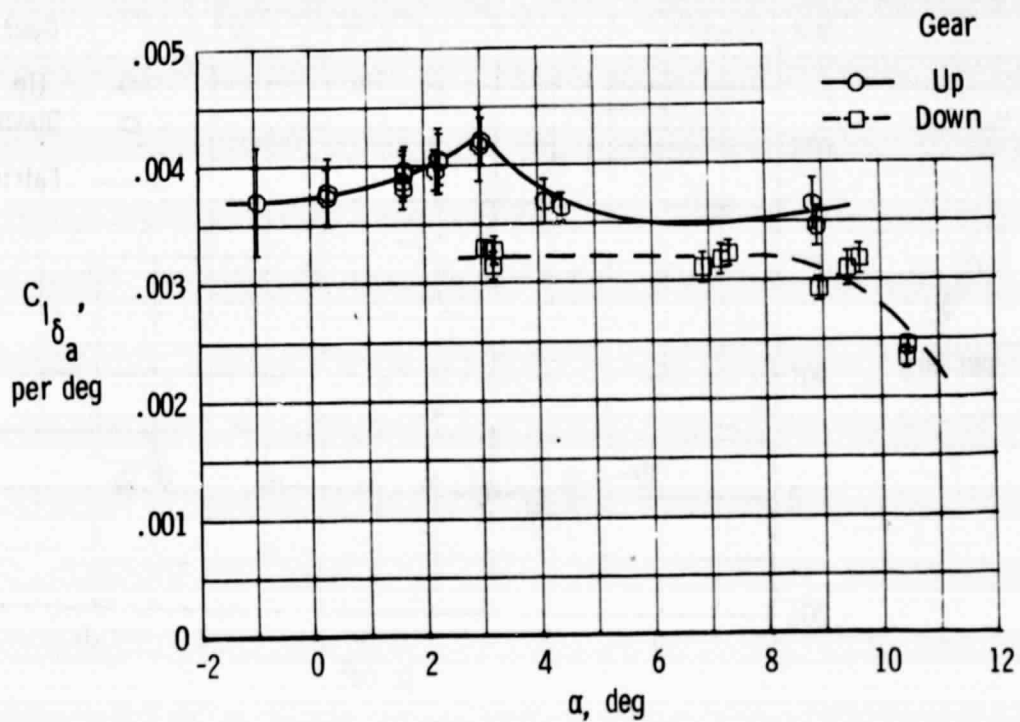
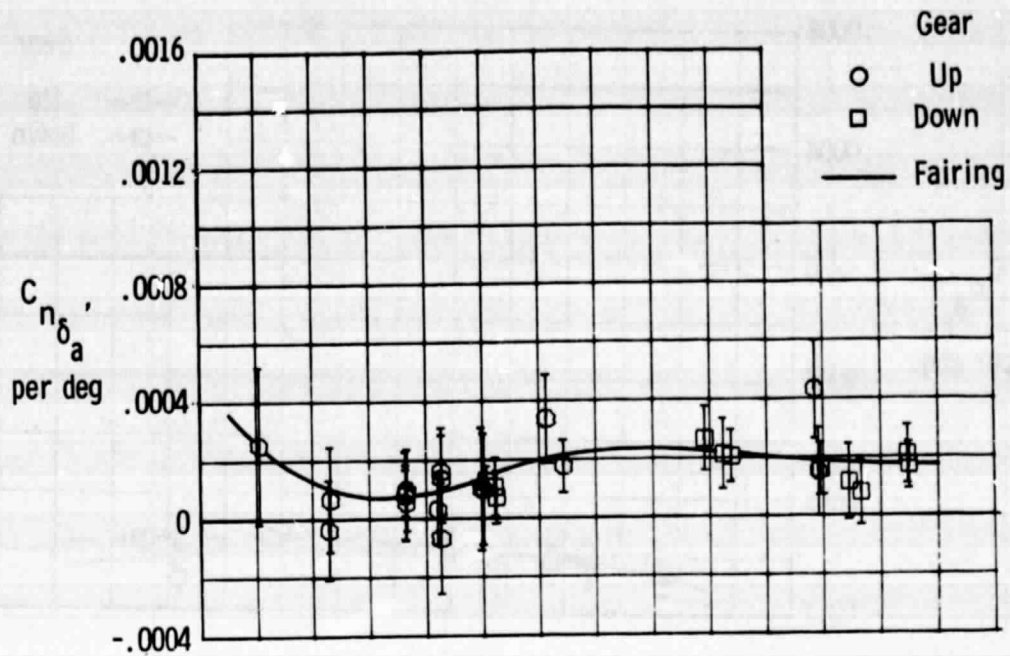
(e) C_{l_p} , C_{n_p} .

Figure 5. Continued.



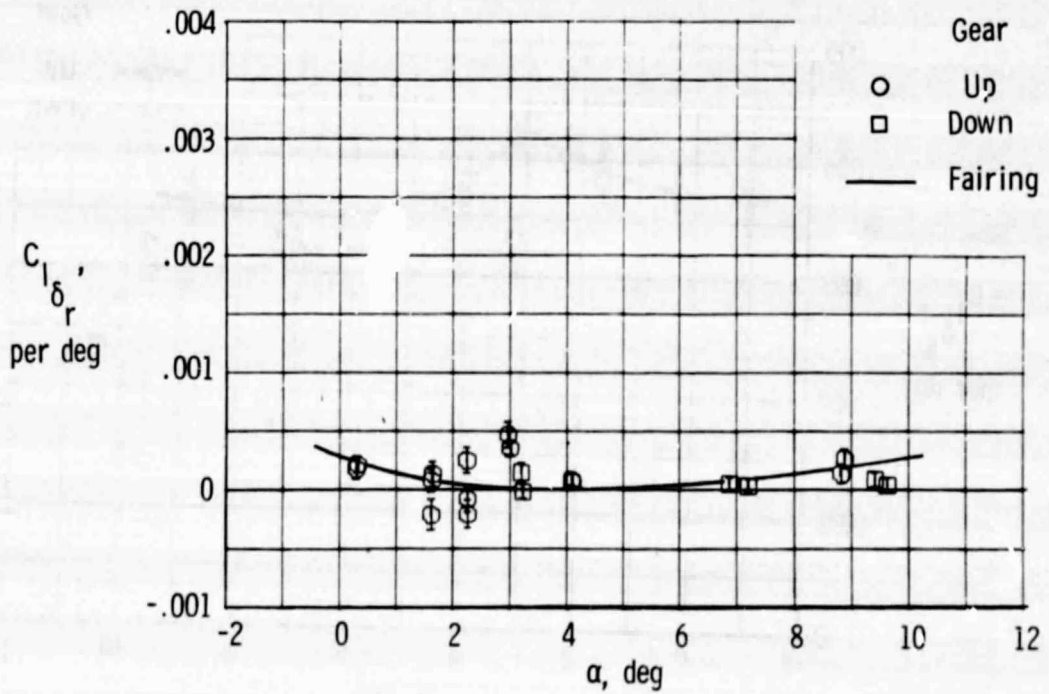
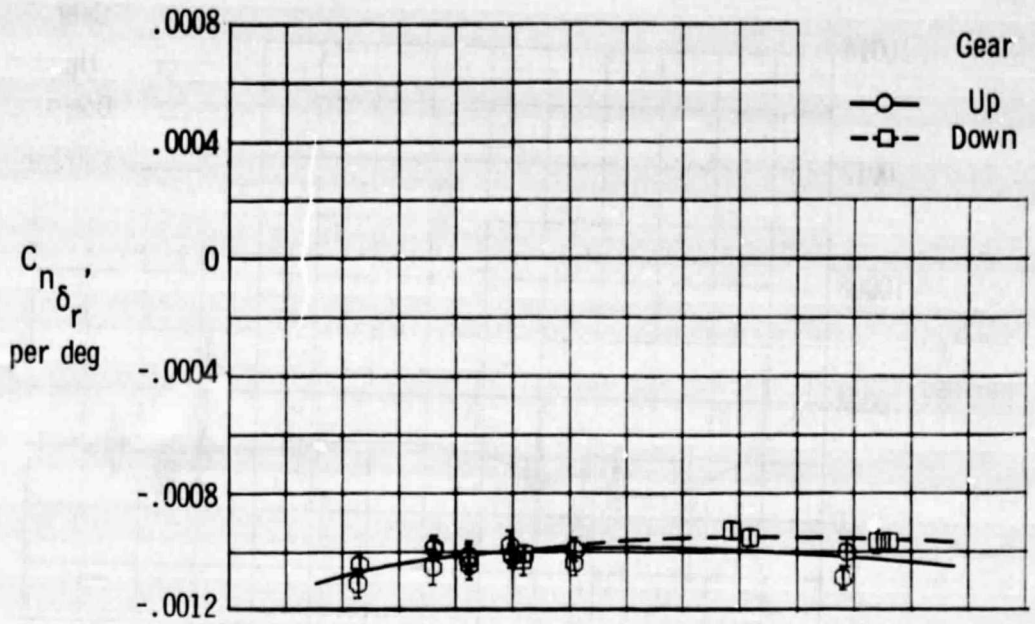
(d) C_{n_r}', C_{l_r}' .

Figure 5. Continued.



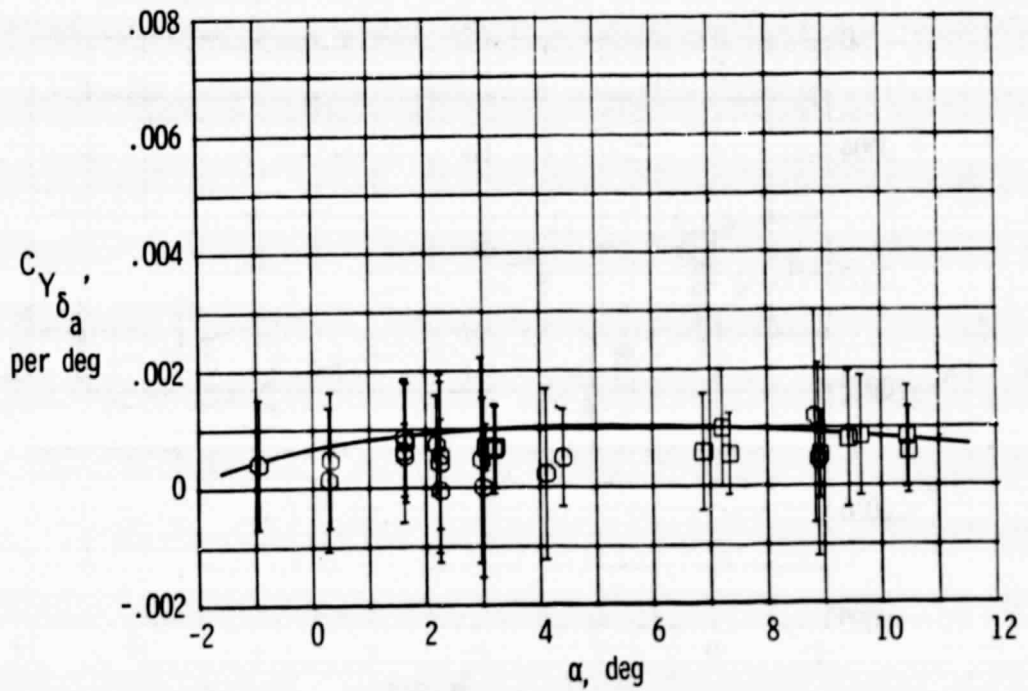
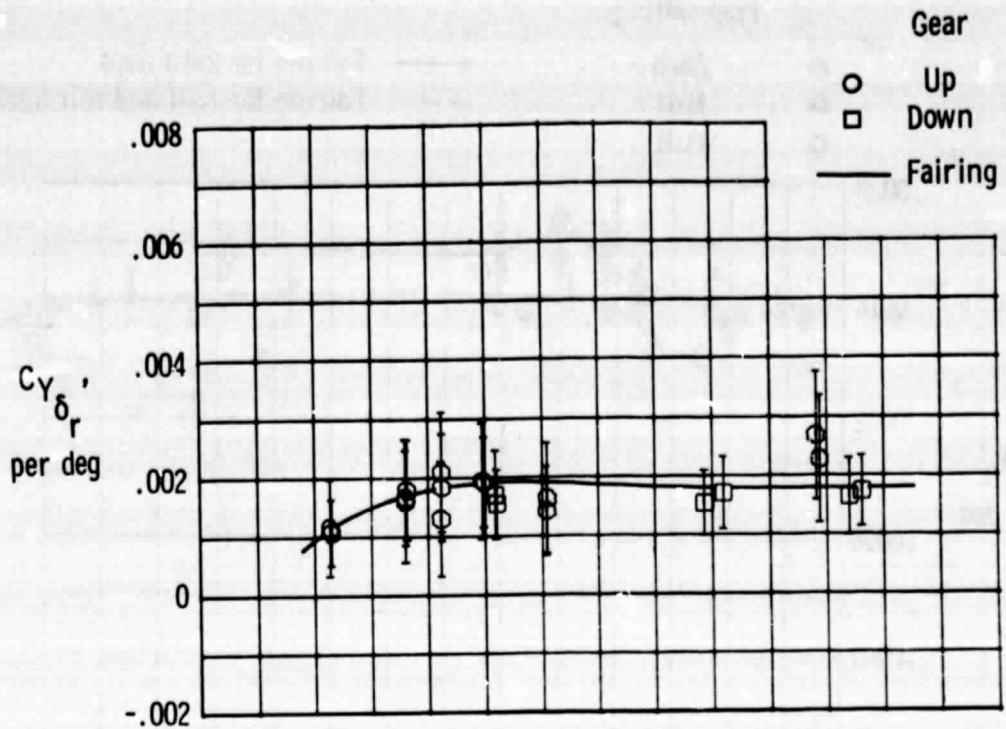
(e) $C_{n_{\delta_a}}, C_{l_{\delta_a}}$

Figure 5. Continued.



(f) $C_{n\delta_r}$, $C_{l\delta_r}$

Figure 5. Continued.



(g) $C_{Y\delta_r}$, $C_{Y\delta_a}$

Figure 5. Concluded.

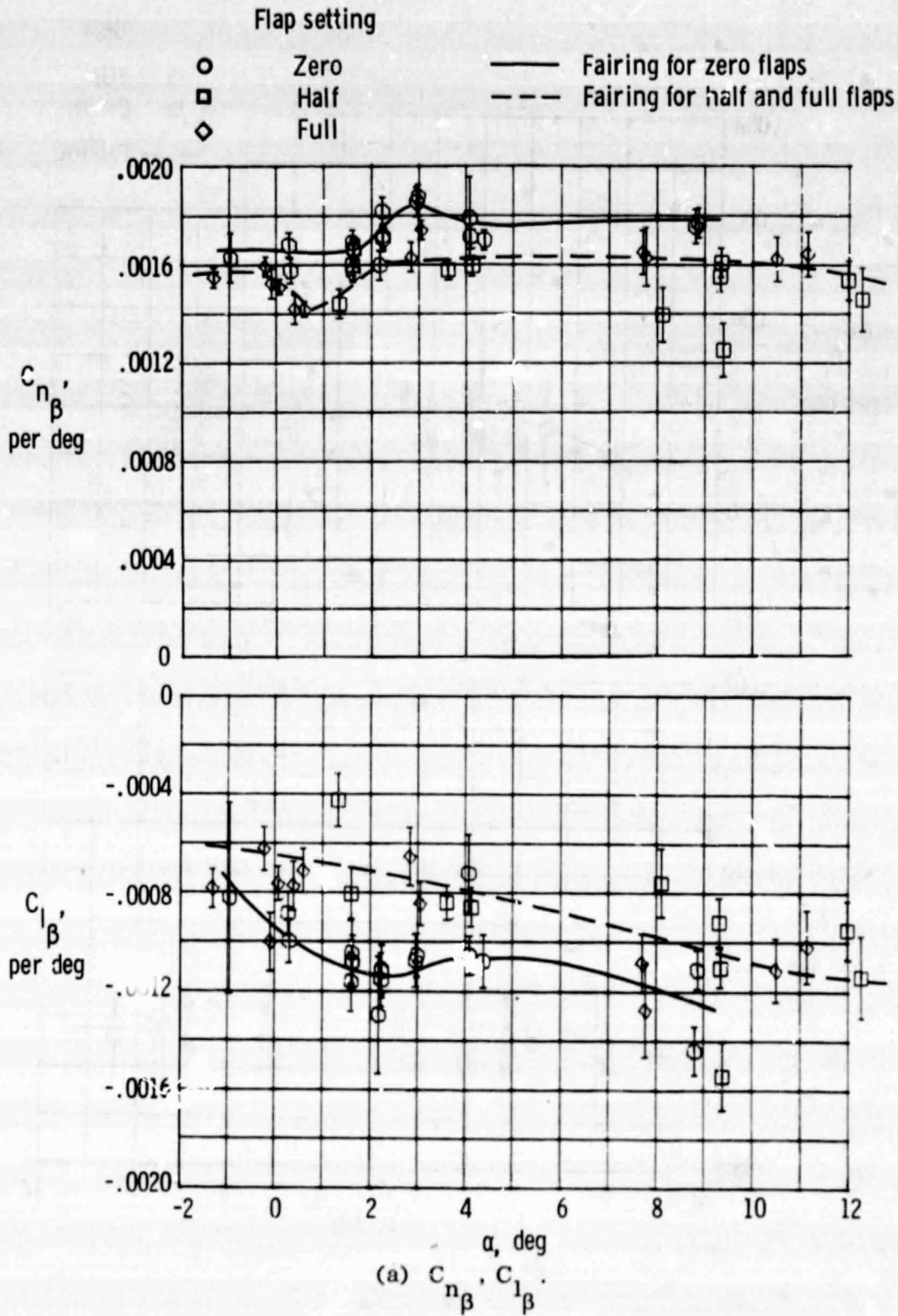
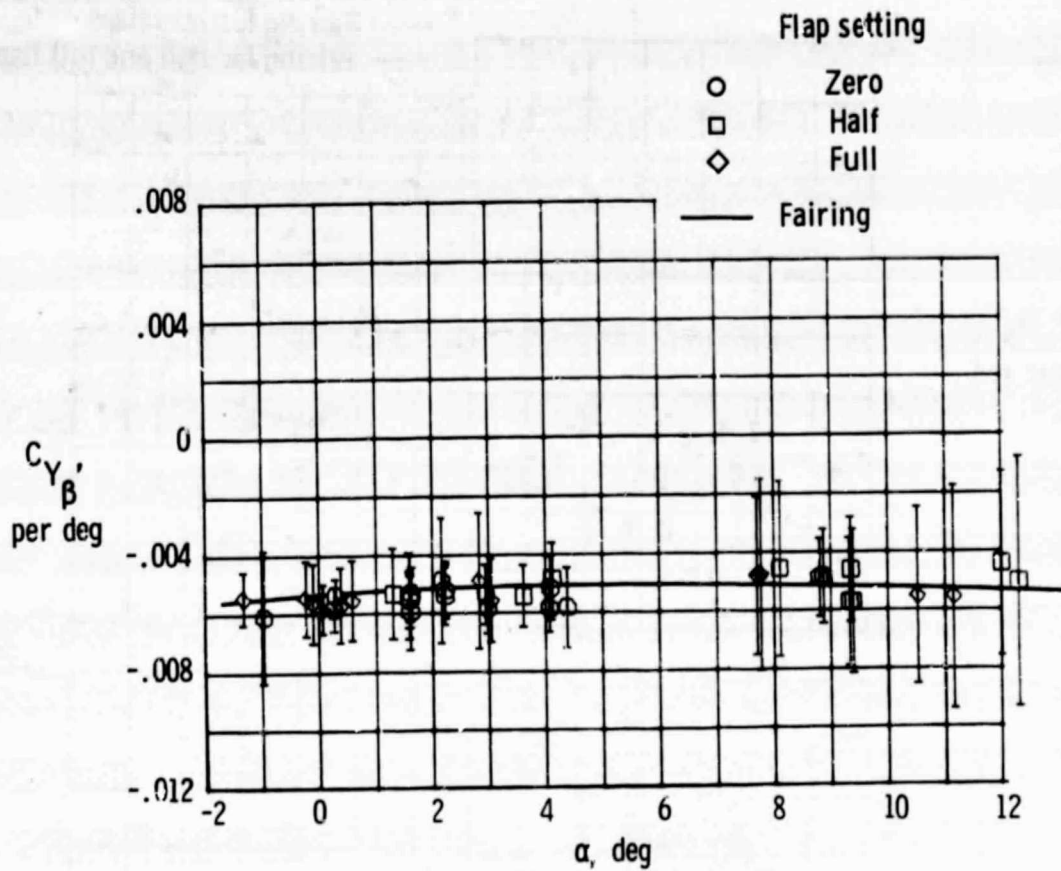


Figure 6. Lateral-directional stability and control derivatives for gear up configurations.



(b) $C_{Y\beta}$.

Figure 6. Continued.

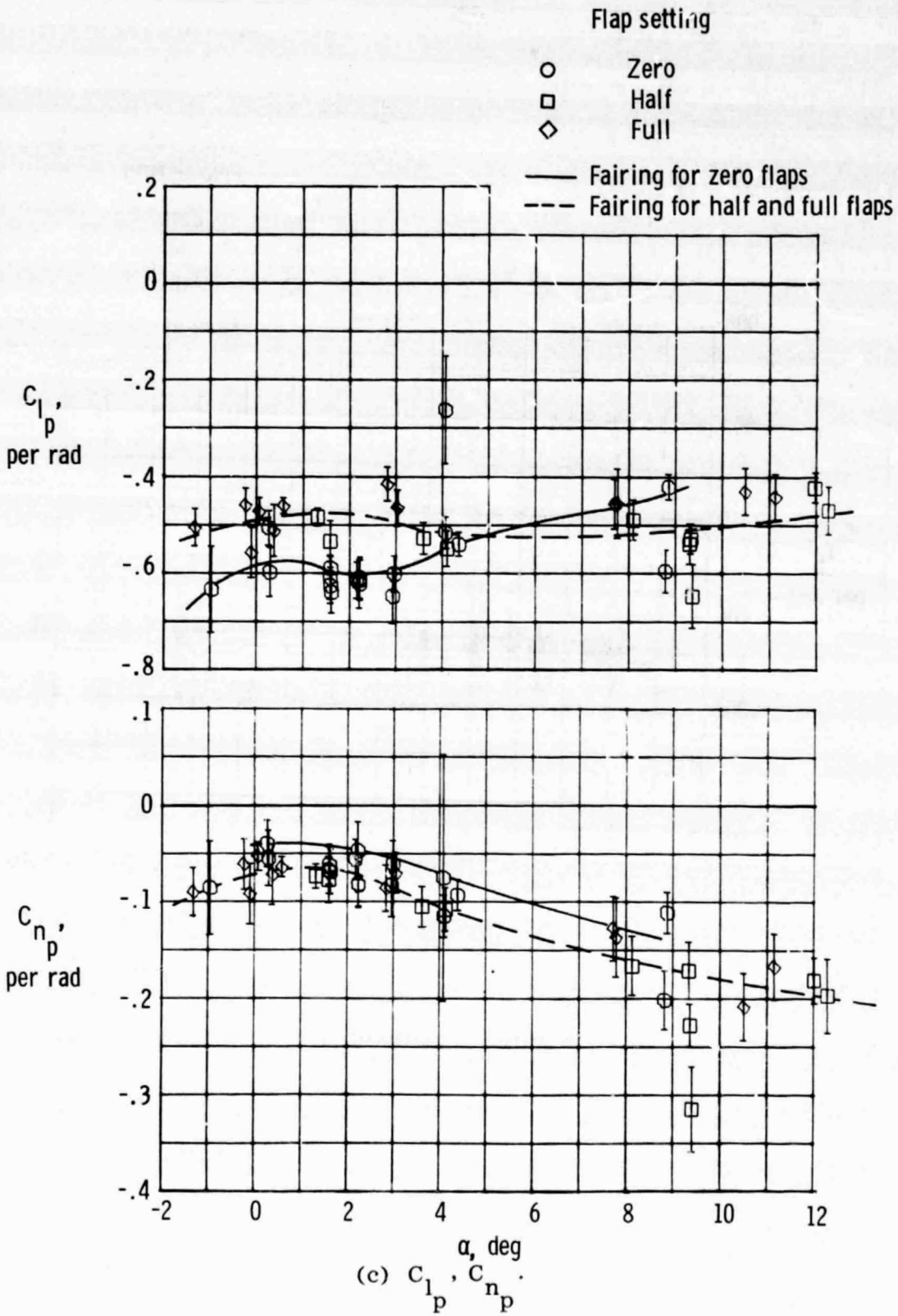
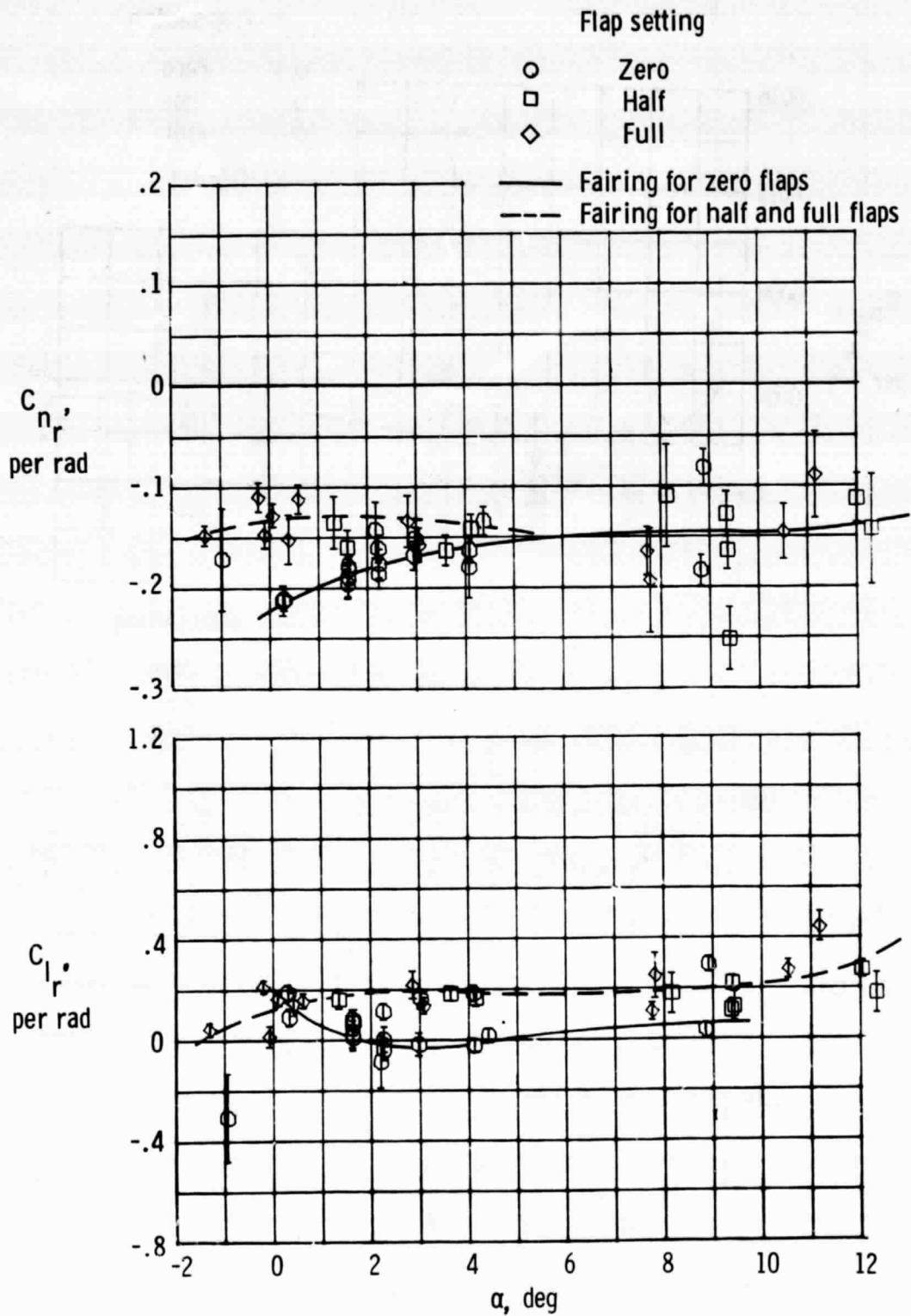
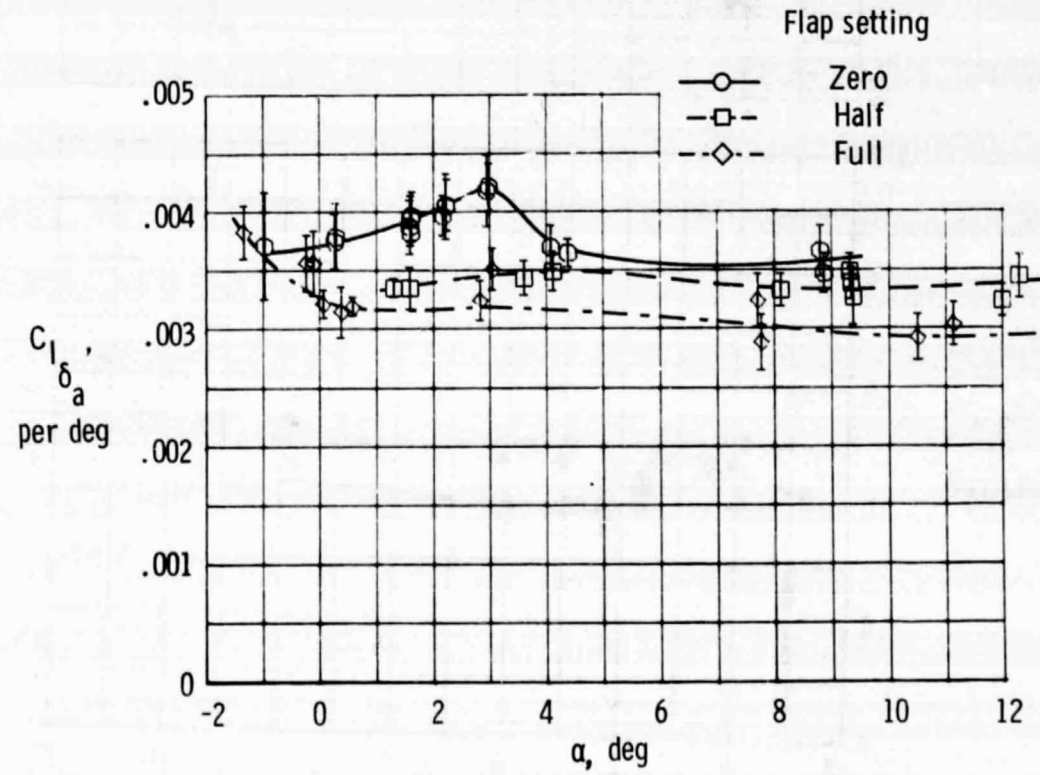
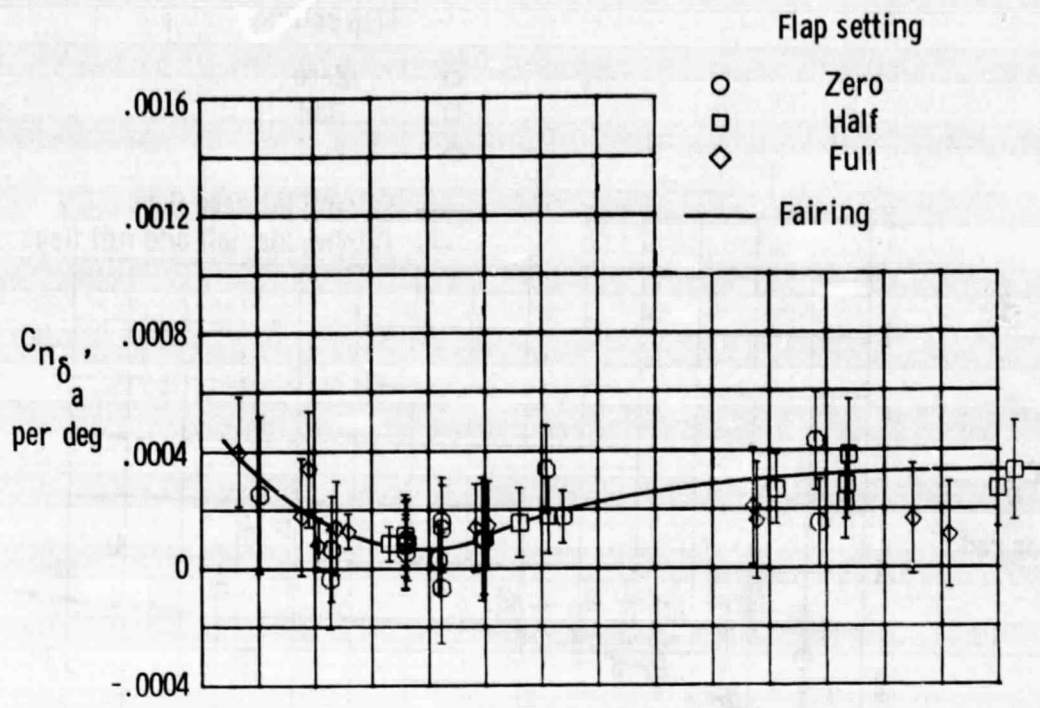


Figure 6. Continued.



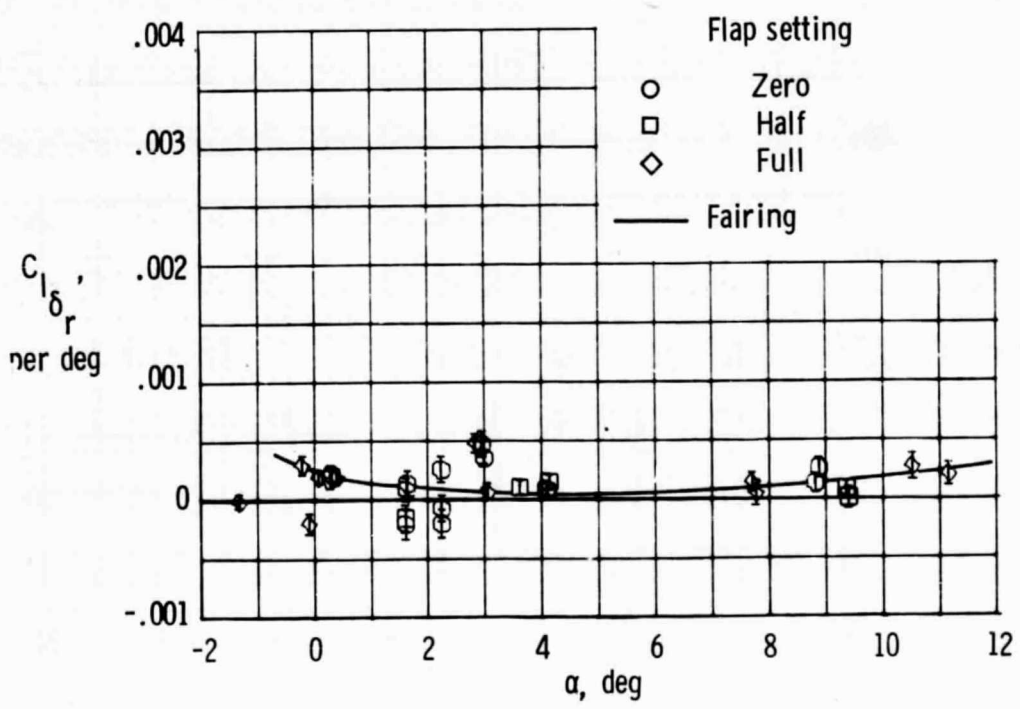
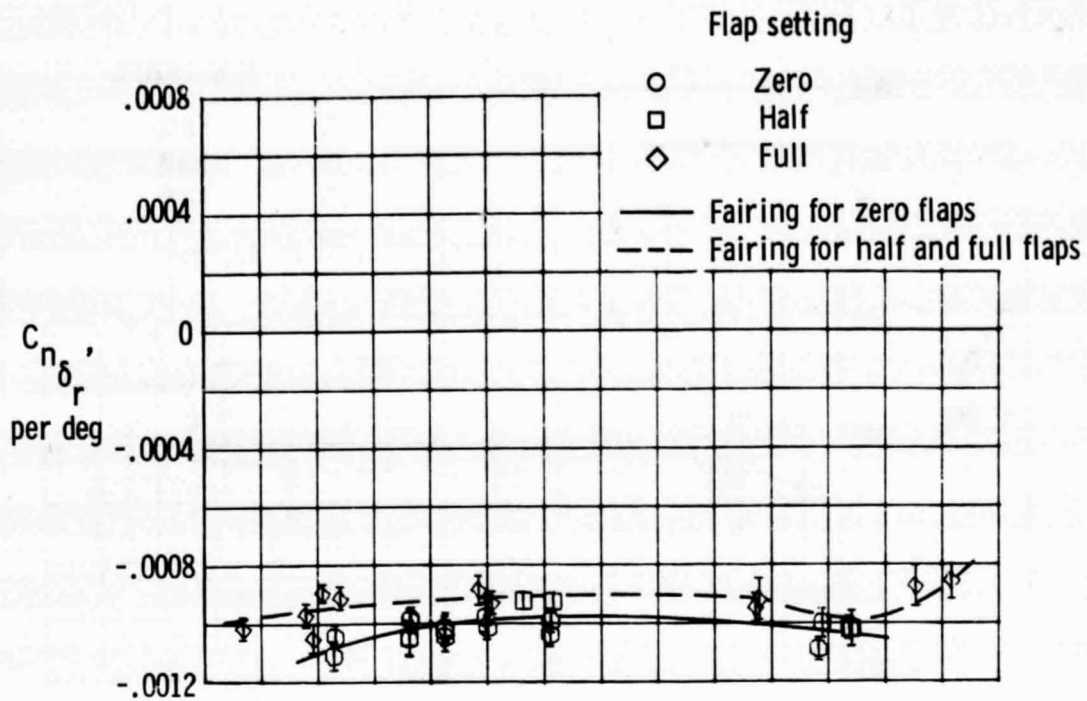
(d) C_{n_r}, C_{l_r} .

Figure 6. Continued.



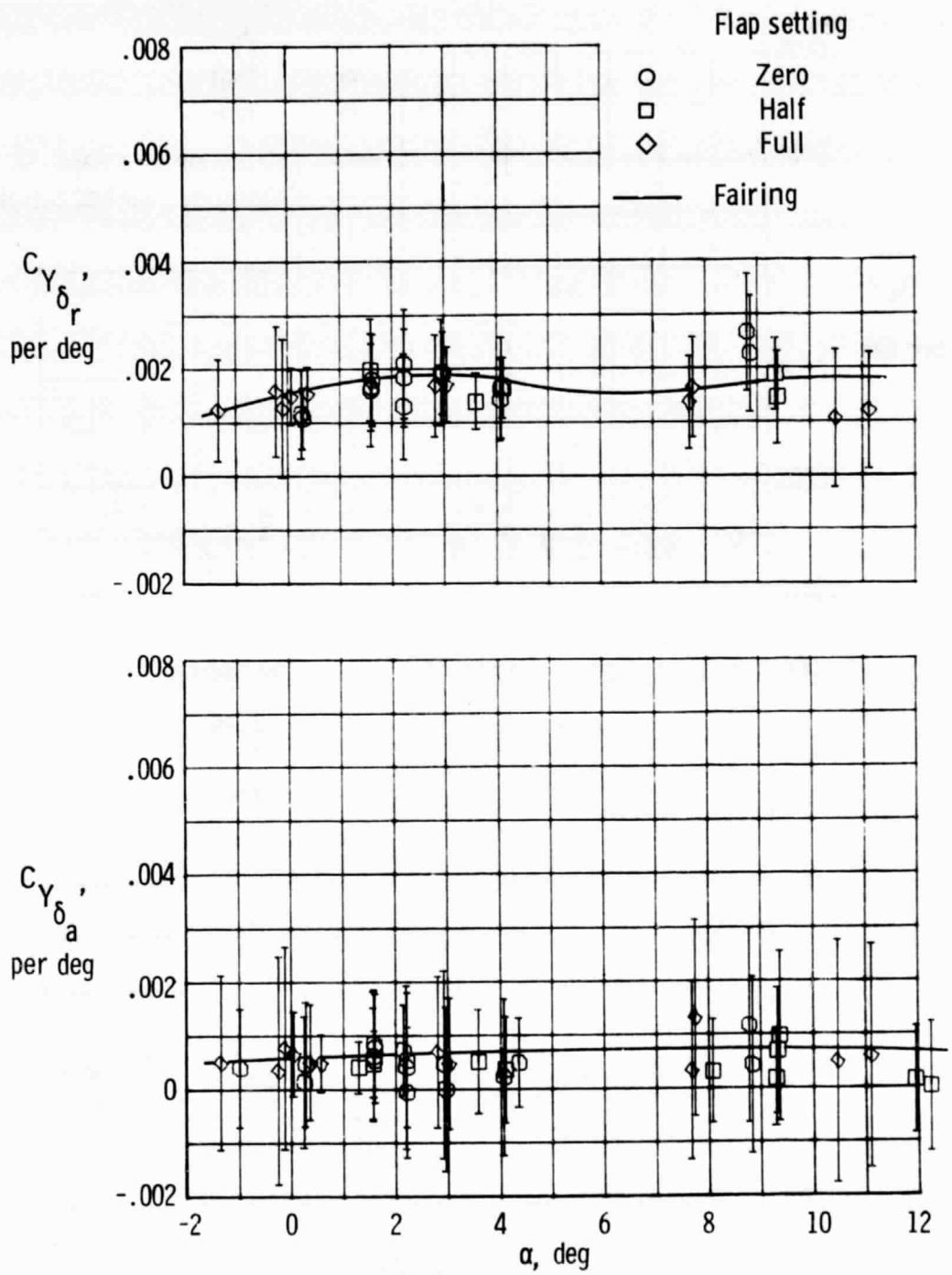
(e) $C_{n\delta_a}$, $C_{l\delta_a}$

Figure 6. Continued.



(f) $C_{n\delta_r}, C_{l\delta_r}$

Figure 6. Continued.



(g) $C_{Y\delta_r}$, $C_{Y\delta_a}$

Figure 6. Concluded.